PREDICTION OF METAL PM EMISSION IN RAIL TRACKS FOR CONDITION MONITORING APPLICATION

Belachew Tesfa*, Fengshou Gu, Arthur Anyakwo, Faisal Al Thobiani, Andrew Ball
*Centre for Diagnostic Engineering, University of Huddersfield, UK, b.c.tesfa@hud.ac.uk, +44 (0) 1484 473532

Keywords: Railways, Metal particle emission, Emission prediction, Wear models.

Abstract

Exposure to particulate material (PM) is a major health concern in megacities across the world which use trains as a primary public transport. PM emissions caused by railway traffic have hardly been investigated in the past, due to their obviously minor influence on the atmospheric air quality compared to automotive transport. However, the electrical train releases particles mainly originate from wear of rails track, brakes, wheels and carbon contact stripe which are the main causes of cardio-pulmonary and lung cancer. In previous reports most of the researchers have focused on case studies based PM emission investigation. However, the PM emission measured in this way doesn't show separately the metal PM emission to the environment. In this study a generic PM emission model is developed using rail wheel-track wear model to quantify and characterise the metal emissions. The modelling has based on Archard's wear model. The prediction models estimated the passenger train of one set emits 6.6mg/km-train at 60m/s speed. The effects of train speed on the PM emission has been also investigated and resulted in when the train speed increase the metal PM emission decrease. Using the model the metal PM emission has been studied for the train line between Leeds and Manchester to show potential emissions produced each day. This PM emission characteristics can be used to monitor the brakes, the wheels and the rail tracks conditions in future.

1 Introduction

Particulate matter (PM) emissions from the transport sector become a major health concern for the last decades. The effects of elevated level of PM, particularly fine PM or $PM_{2.5}$ (particle with less than 2.5 aerodynamic diameter), and their adverse human health effects has been well reported[1–4]. The composition of PM is very complex and is heavily dependent on local sources and metrology. Due to the stringent emission law, the PM emissions of automotive sectors are well investigated and documented. The PM effects on health, their size distribution, the correlation with metrology, the fuel type effects and reduction mechanism have been reported well[5–9]. Comparing the light duty vehicles, trains have obviously negligible aerosol emissions per passengers and km. Due to this, in many countries the public transportation by railway systems is highly promoted especially in urban areas, to reduce the individual vehicles [10].

Most of the published papers focused on in-train exposure to air pollutants or on in-train exposure to air pollutants or measurement of PM in sub way systems. Recently, Kam et al. [3] carried out an extensive PM sampling campaign in May – August 2010 to measure PM emission of underground subway line and a ground level light-rail line. Their objectives were to determine personal PM exposure of commuters of both lines and to compare the PM emission concentration at platform and inside the train. It found that the subway commuters were exposed on average to PM_{10} and $PM_{2.5}$ concentrations that were 1.9 and 1.8 times greater than ground level commuters. The average PM_{10} concentrations for the subway line at station platforms and inside the train were 78.0μg m^{-3} and 31.5μgm^{-3}, respectively; for the light-rail line, corresponding PM_{10} concentrations were 38.2μgm^{-3} and 16.2μgm^{-3}. Similar investigation has been conducted in Stockholm undergrounds by Johansson and Johansson[4]. They reported that during week days between 7a.m. and 7p.m. the average PM_{10} and $PM_{2.5}$ concentrations were 470 and 260μgm^{-3}, respectively. The underground level of emission is 5 and 10 times higher than the corresponding values measured in one of the busiest streets in Central Stockholm. The particles emitted from trains in Switzerland due to the material losses from brakes, wheels, etc. have been estimated by Burkhardt et al.[11] for 7200km tracks. They found that the emission compose about 2270 ton per year metals, 1357ton per year hydrocarbons and 3.9ton per year herbicides. Most of the released metals are particles emitted by friction processes with iron, followed by copper, zinc, manganese, chromium and nickel. Similarly, Fridell et al.[1] measured the emission of metals and reported the freight trains, commuter trains and regional trains emit 2.9g/train-km, 0.48g/train-km and 0.24g/train-km respectively. In 1999, Pfeifer and colleagues [12], investigating metal concentrations in the blood of London commuters, noted that the underground user was particularly enriched in Mn, approximately 10-fold, when compared to the Mn in the general environment. They concluded that the Mn source for the underground user is the metal PM emission from the train system. Seaton et al.[13] investigated the hazardous associated with exposure to dust in the London Underground railway, they found that the dust comprised by mass approximately 67% is iron oxide and 1-2% quartz[13].

Currently, as most trains in developed countries are run by electric power sources, the only direct particulate emission occur by different forms of material wear i.e. from tracks, wheels, brakes and the overhead traction line and vaporization of metals due to sparking [4,10]. As reviewed

above, most of the studies on PM emission from rail way systems have been focus on the general emission of PM emission which includes particles from the road, near by construction and others. The PM emission from these measurements could not show the metal emission separately. Comparing the metal with other particulate matters, the former one is very dangers to health as it is easy to enter into respiratory system. In addition, there is lack of metal PM emission prediction models which give an opportunity to analysis the train emission system quickly and a cost effective way by means of simulations, in contrasts to lengthy and expensive field or laboratory measurements. Therefore, this study is to develop metal PM emissions using wear model of rail track and wheel system as well as recommending ways of using the metal PM emission for condition monitoring. This prediction model will have multi applications:

1. It can be used to estimate the metal PM emission at ground and underground tracks. It will help to develop a remedy system to reduce the metal PM emission.
2. The model also can be used to estimate the wear on rail and wheel to provide basis for planning maintenance work.
3. The new wheel materials and lubrications can be investigated with less time and in a cost effective way by using wear simulations, in contrast to lengthy and expensive field or laboratory measurements.

2 Metal PM Emission Predication Models

The metal PM emission from railway comes from the wear of the tracks, wheels and brakes. The wear is determined by measuring the wear depth or volume. Bolton et al. [14] made a classification between mild and severe wear based on wear rate, roller surface appearance, metallographic features of roller sections, and wear debris. In the case of relatively low levels of normal contact stress and creepage, mild wear in the form of a nearly continuous oxide film was observed on the roller surfaces. In the severe wear mode, metal flakes were developed. In wheel-rail application, severe wear is mostly present on the wheel flange and on the rail gauge corner. The severe mode contributes for the metal PM emission.

To predict the wear, several models have been proposed. Archard[15] proposed in 1953, the volume (V_{wear}) of removed material is proportional to the normal load and sliding distance as expressed in equation(1):

$$V_{wear} = K_1 \frac{F_Z S}{H} [m^3] \quad (1)$$

Where *Fz [N]* is the normal wheel-rail contact force, *S[m]* is the sliding distance in the contact patch, $H[N/m^2]$ is the hardness of the softer material and K_1 is a non-dimensional wear coefficient. Archard's wear model has been used in wheel-rail applications although the principle cause of wheel/rail wear is rolling and not pure sidings.

Another approach [16] stems from the assumption that the removed material volume is proportional to the frictional work in the contact patch. The frictional work per metre rolled distance is calculated as a sum of products containing the tangential forces and spin moment and the corresponding creepages in the wheel-rail contact. In this case, the wear index w_i is expressed as

$$W_i = K_2(F_x\gamma_x + F_y\gamma_y + M_z\emptyset_z \quad (2)$$

Where *Fx, Fy* and *Mz* are the longitudinal and lateral creep forces and the spin moment, while γ_x, γ_y and γ_z are the corresponding creepages.

Ward et al[17]. performed twin disc tests to determine wear rates to be used in a wheel transverse profile wear model that is based on the frictional work hypothesis. Wear rate W_r, in terms of removed mass per metre rolled distance and per mm^2 contact area, was calculated as

$$W_r = K_i \frac{T\gamma}{A} [\left(\frac{\mu g}{m}\right) / mm^2] \quad (3)$$

with *T [N]* is creep force, *γ [-]* is creepage, $A\ [mm^2]$ is contact patch area and K_i *(i=1, 2 ,3)* [μg/Nm] wear coefficient.

In this study the Archand's wear model have been selected to predict the metal PM emission. The Archard's model Equation 1 have been selected because of the flexibility of parameters in the equation to consider the rail operation conditions such as rail speed, time elapse, distance covered and load applied.

3 Methodology

The wear and rolling contact fatigue of wheel and rail depends greatly on their profiles and contact surface status, the geometry sizes of track and dynamical behaviour of railway vehicle coupled with the track. The dynamic simulation the rail-wheel contact has been developed using wheel-rail contact model to determine the wheelset geometry parameters, the normal contact forces, the tangential contact problem and the dynamic behaviour of the wheelset on the track. The equations which used to in wheel–rail contact model simulations are presented in Appendix A. The flow diagram of the simulation which has been used in this model has been shown in Figure 1. The first block diagram describes the wheelset geometry. Here the inputs are the wheel-rail material physical properties, the lateral displacement, roll angle, yaw angle wheelset nominal rolling radius, and the rail radius dimensions. The wheel and rail profiles are parameterized using piecewise cubic interpolation polynomial.

The minimum difference method [18] is applied to find the difference between the wheel profile contact position and the rail profile contact position. The wheel-rail contact coordinates solutions are checked for indentation. If the indentation is negative, then the solution is disregarded and re-computed to calculate the actual wheel-rail contact coordinates. If the wheel-rail contact co-ordinates is negative or zero, then the wheel-rail contact coordinate is saved and used for implementation in the wheelset dynamic model.

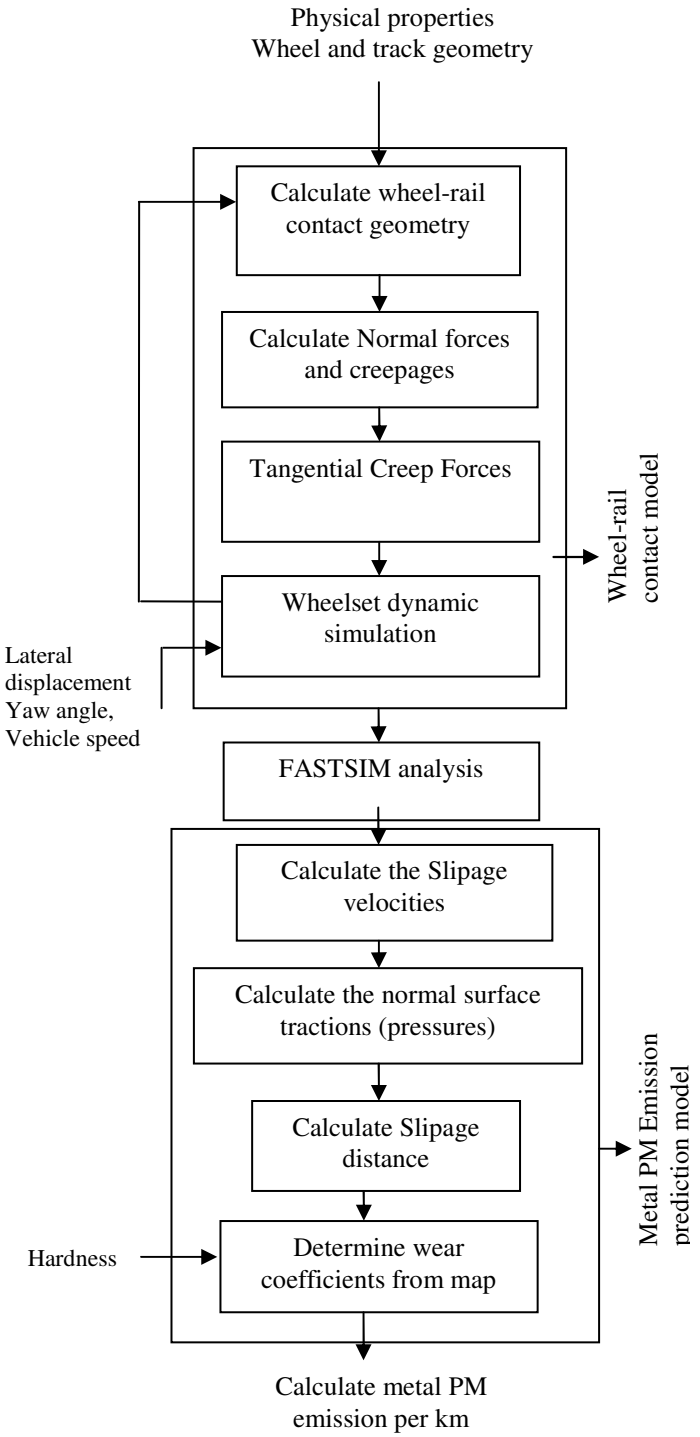

Figure 1 Methodology of metal PM emission wheel-rail system

Once, the wheel-rail contact points are determined, they are used to calculate the rolling radius difference function and the contact angle function. The interpolated values of the rolling radius difference are used to calculate in the tangential contact problem block to calculate the creepages, creep coefficients and the creep forces developed in the wheel-rail contact patch. The contact angle function is also used simultaneously in the normal contact problem block to calculate the normal contact forces acting on the wheel-rail interface. The normal forces calculated are then used to determine the size, shape and orientation of the wheel-rail contact patch using Hertz contact theory. The contact patch size dimensions are assumed to be elliptical in shape. The elliptical Hertzain contact area is used in FASTSIM for establishing the grid. The contact ellipse in the present implantation of the FASTSIM algorithm is divided into 81x81 elements to provide smooth wear distributions. The relative velocity (slip velocity) for steady-state rolling and linear elasticity is defined as equation (4) as described by Jendel [19].

$$\overline{v_{slip}} = V_{train}\left[\begin{pmatrix} v_x - \emptyset y \\ v_y + \emptyset x \end{pmatrix} - \frac{\partial \bar{u}(x,y)}{\partial x}\right] \quad (4)$$

Where T_{train} is the vehicle speed (m/s), v_x the longitudinal creepage, v_y the lateral creepage, $\emptyset$ the spin creepage(1/m), $\bar{u}$ the elastic displacement(m), and x, y the cartesian coordinates of the contact ellipse (m).

Since the rigid slip term is usually much larger, it is not a severe limitation to neglect the elastic part in FASTSIM. The magnitude of the sliding distance (s) is then computed by multiplying the slip velocity with the time for each element in contact with the rail in longitudinal direction by equation (5). The slip distance has been used in metal PM emission prediction in equation (1).

$$S = \left|\bar{v}_{slip}\right| \frac{\Delta x}{V_v} \quad (5)$$

Where Δx is the longitudinal element length

The wear coefficient (K) has been estimated using the contact pressure and sliding velocity. Jendel proposed wear coefficient map shown in Fig. 2. Jendel [17] wear coefficient map was based on experimental results for wheel and rail made of steel.

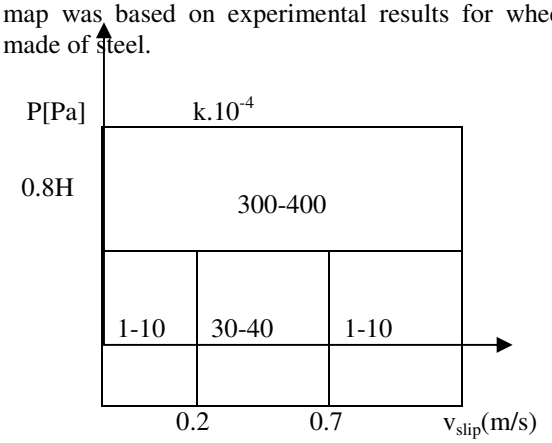

Figure 2 wear chart for the wear coefficient k based on laboratory measurements with wheel and rail steels [19]

After generic metal PM emission model developed, the model has been applied to passengers train operating between Leeds and Manchester. This line is mainly operating by First TransPennine Express. The line has five stopping station including the Leeds and Manchester. The train work between

00:53 to 23:38 on Monday to Saturday with 64 trains' trip from Leeds to Manchester and 63 trips from Manchester to Leeds. On Sunday the numbers of trips are reduced to 43 from Leeds to Manchester and 44 for Manchester to Leeds. The train pass almost in 15 min during rush hours and normal time. The rail network is shown in Figure 3. In this simulation the irregularities and curvatures have not consider in the line. The total distance between Leeds and Manchester is about 69Km. In the metal PM emission prediction, the length of the train has been considered for different interval of time. This particular choice of line selected due to the uniform traffic situation, which have notably effects in wear modelling.

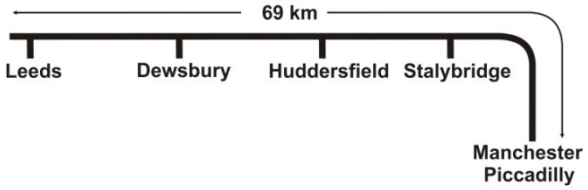

Figure 3 Leeds to Manchester line

4. Results and Discussion

In this study the metal PM emission models has been developed using the Archard's wear model. The simulations have been done for a range of train speeds such as 20m/s(73km/h), 40m/s(146km/h) and 60m/s(219km/h).

Figure 4(a) shows that metal PM emission at train speed of 20m/s for both right wheel and left wheel at same time. It can be seen that when the lateral displacement is shifted to the right the metal PM emission from the right wheel is higher than that of left wheel as it is expected. The effects of train speed on the PM emission have been shown in Figure 4(b). It can be seen that when the train speed increases, the metal PM emission decreases. Considering the average train speed (60m/s) as reference, the metal PM emission increases by 28% and 10% for 20m/s and 40m/s respectively. This can be explained when the vehicle speed reduced, the contact retention time between the wheel and track increases, as result the wear between the two surface increase, consequently the metal PM emission increase.

The depth of the wheel removed by wear has been calculated from the volume of wear and contact area of wheel and track and is shown in Figure 5. Similar to the metal PM emission when the train speed increases the depth of wear also increases on the wheel.

The metal PM prediction model has been used to predict the PM emission of train for one day journey between Leeds and Manchester as case study. Figure 6(a) shows the number of trains journeying between Leeds and Manchester. As it can be seen from the bar graph from 8 to10 and 16-18 are the peak times. During the time between 10-16 there is almost the same number of trains .

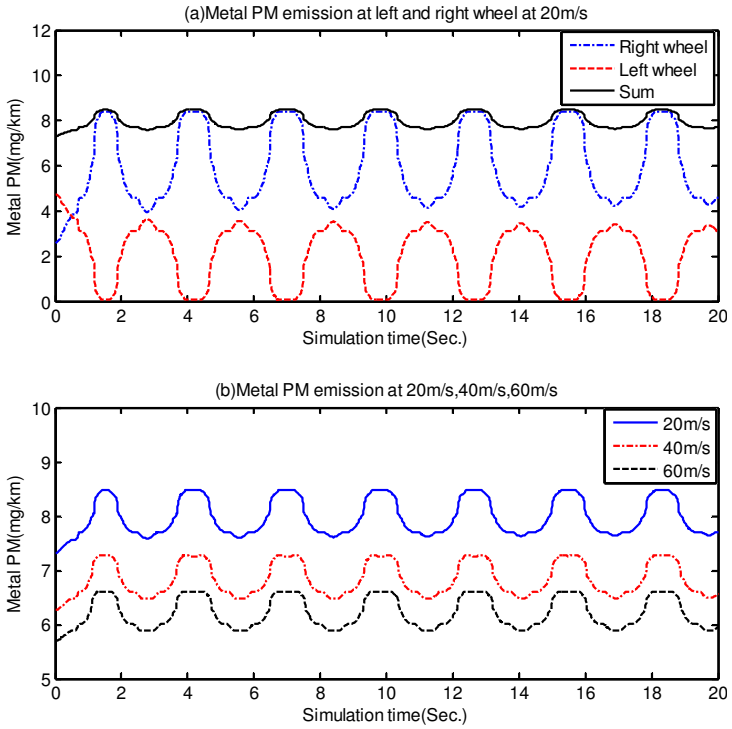

Figure 4 (a) Metal PM emission at 20m/s for both left and right wheel (b) Metal PM emission at range of vehicle speed

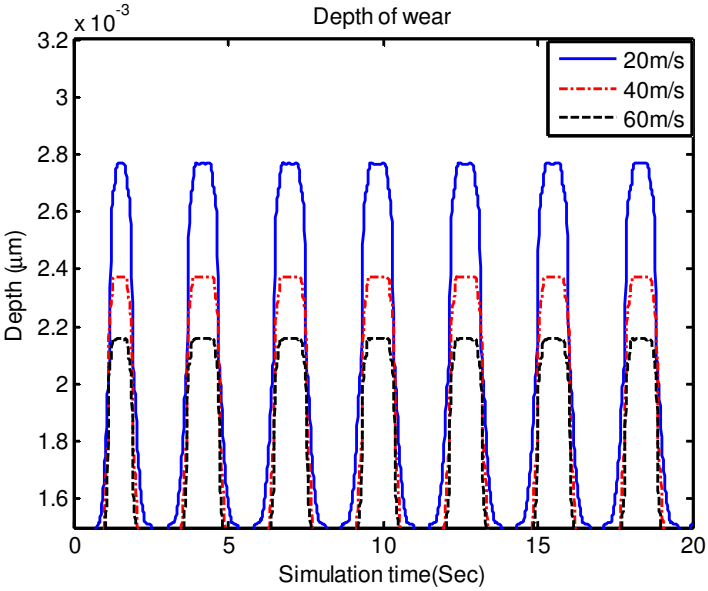

Figure 5 Depth of wear on wheel

By taking into account the number of trains journeying between Leeds and Manchester the metal PM emission have been predicted and presented in Figure 6(b). Corresponding to each travel time the metal PM emission has been predicted. As expected, the time period with higher number of trains and larger size of trains emit higher metal PM. The journey between Leeds and Manchester emits maximum metal PM emission of 73g during peak time i.e.16 to 18. The train line between Leeds to Manchester emits 372g of metal per day.

.

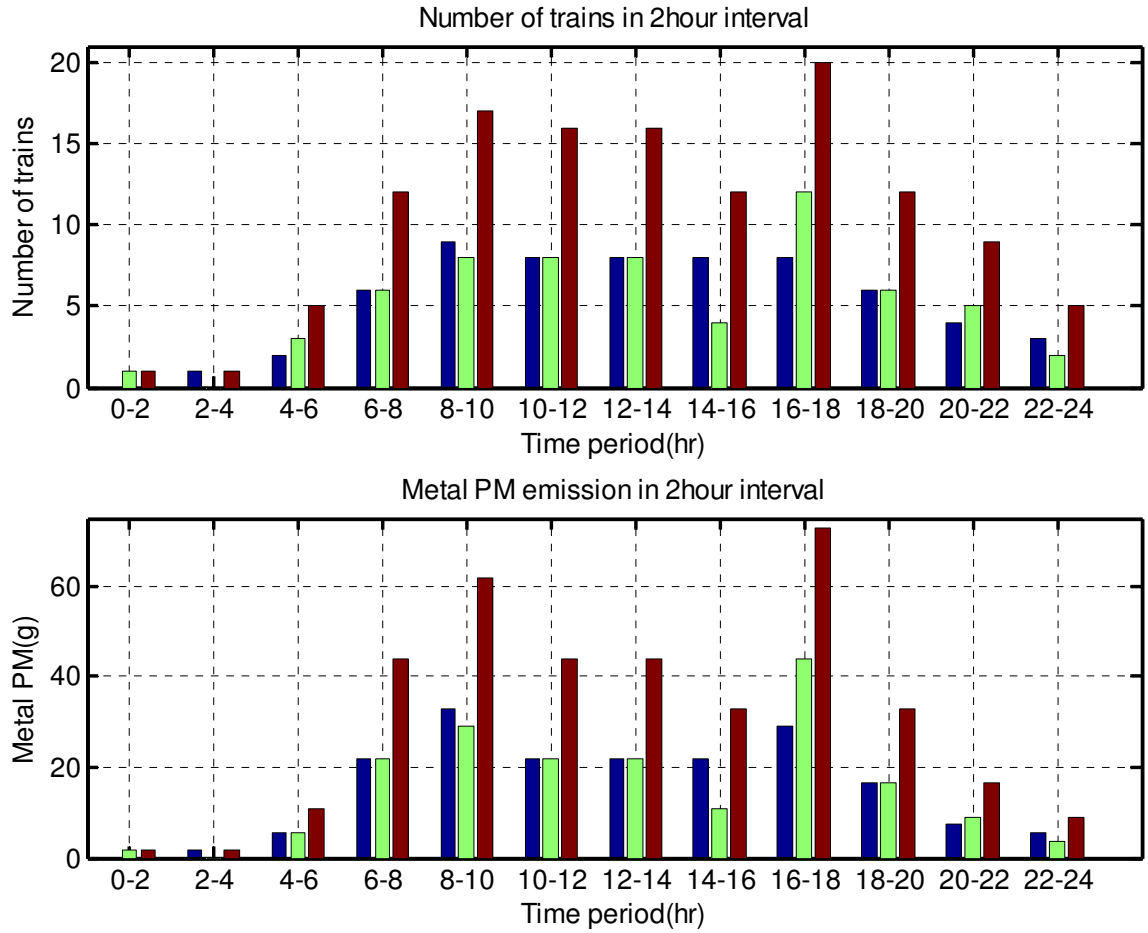

Figure 6 (a) Number of trains from Leeds to Manchester and Manchester to Leeds (b) Metal PM emission from train journeying between Leeds to Manchester per day

5. Conclusions

In this study a generic PM emission model is developed using rail wheel-track wear model to quantify and characterise the emissions. The prediction models predicted the passenger train of one coach emits 6.6mg/km-train at 60m/s speed. The effects of train speed on the PM emission has been also investigated and resulted in when the train speed increases the metal PM emission decrease. Using the model the metal PM emission has been predicted for the train journeying between Leeds and Manchester Piccadilly for one day trip. The journey between Leeds and Manchester emits metal PM emission of 372g per day at 60m/s speed. This metal PM emission characteristics can be used to monitor the brakes, the wheels and the rail tracks conditions in future. The future work of this study primarily focus on making the prediction model more robust and general and developing condition monitoring tools using the metal PM emission which can be integrated with train near to the wheel.

Appendix A: Contact model equations

Hertz contact theory predicts the size of the contact patch using as follows

$$ab = mn\left[\frac{3(1-u^2)}{2E(A+B)}N\right]^{2/3} \qquad \text{(A1)}$$

where m and n are the Hertz elliptical constants [2], N is the normal force (left and right wheel-rail) acting on the contact patch and A and B are the relative curvatures of the wheel and rail, E is the Young Modulus of steel and u is the Poisson's ratio. The expressions for the relative curvature of the wheel and rail are defined as follows;

$$A = \frac{1}{R}, \qquad B = \frac{1}{R_{rail}} \qquad \text{(A2)}$$

Normal contact pressure

The semi-ellipsoidal normal pressure distribution can be computed by using the relationship

$$P_z(x,y) = \frac{3N}{2\pi ab}\sqrt{1-(x/a)^2-(y/b)^2} \qquad \text{(A3)}$$

The maximum normal contact pressure occurs at the centre of the contact patch when x = y = 0. At this point the maximum normal contact pressure can be expressed as

$$P_m = \frac{3N}{2\pi ab} \qquad \text{(A3)}$$

Creepages

The dynamic wheel-rail contact creepages developed at the contact patch for the right and left wheel-rail contact are described as follows;
The longitudinal creepages at (right and left) wheel-rail contact

$$v_{xr} = \frac{v(1 - R_r/R_0) - l_0\dot{\psi}}{v}, v_{xl} = \frac{v(1 - R_l/R_0) + l_0\dot{\psi}}{v} \quad \text{(A4)}$$

The lateral creepages at the right and left wheel-rail contact

Appendix B: Nomenclature

l_0 = Half wheel axle length to the contact point (752.425mm)
G = Shear Modulus of rigidity = $80x10^3$MPa
$\dot{\varphi}$ = Roll velocity (mm/s)
ψ = yaw angle (radians)
$\dot{\psi}$ = yaw velocity (rad/s)
R_0 = Nominal rolling radius of the wheel (460mm)
R_l = Left wheel rolling radius (mm)
R_r = Right wheel rolling radius (mm)
R_{railL} = Rail radius (304.8 mm)
a = Semi-axes in the longitudinal direction
b = Semi-axes in the lateral direction
I_z = Moment of Inertia of the wheelset ($935x10^6$kg-mm^2)
K_{py} = Lateral suspension stiffness ($4550x10^3$N/mm)
K_{px} = Longitudinal spring stiffness (75000 N/mm)
C_{py} = Lateral damper coefficient (0 Ns/mm)
C_{px} = Longitudinal damper coefficient (0 Ns/mm)
m = Mass of the wheelset (1850kg)
W = Axle load (110KN)
v_x = Longitudinal creepage
v_y = Lateral creepage
v_{spin} = Spin creepage

References

[1] E. Fridell, M. Ferm, A. Ekberg, "Emissions of particulate matters from railways - Emission factors and condition monitoring," *Transportation Research Part D: Transport and Environment*, vol. 15, no. 4, pp. 240-245, Jun. 2010.

[2] H. . Adams, M. . Nieuwenhuijsen, R. . Colvile, M. A. . McMullen, P. Khandelwal, "Fine particle (PM2.5) personal exposure levels in transport microenvironments, London, UK," *Science of The Total Environment*, vol. 279, no. 1-3, pp. 29-44, Nov. 2001.

[3] W. Kam, K. Cheung, N. Daher, C. Sioutas, "Particulate matter (PM) concentrations in underground and ground-level rail systems of the Los Angeles Metro," *Atmospheric Environment*, vol. 45, pp. 1506-1516, Mar. 2011.

[4] C. Johansson, P.-Å. Johansson, "Particulate matter in the underground of Stockholm," *Atmospheric Environment*, vol. 37, no. 1, pp. 3-9, Jan. 2003.

[5] J. Zhang, K. He, X. Shi, Y. Zhao, "Comparison of particle emissions from an engine operating on biodiesel and petroleum diesel," *Fuel*, vol. 90, no. 6, pp. 2089-2097, Jun. 2011.

[6] A. Maiboom, X. Tauzia, J.-F. Hétet, "Influence of EGR unequal distribution from cylinder to cylinder on NOx–PM trade-off of a HSDI automotive Diesel engine," *Applied Thermal Engineering*, vol. 29, no. 10, pp. 2043-2050, Jul. 2009.

[7] A. Sarvi, J. Lyyränen, J. Jokiniemi, R. Zevenhoven, "Particulate emissions from large-scale medium-speed diesel engines: 1. Particle size distribution," *Fuel Processing Technology*, vol. 92, no. 10, pp. 1855-1861, Oct. 2011.

[8] P. Q. Tan, Z. Y. Hu, K. Y. Deng, J. X. Lu, D. M. Lou, G. Wan, "Particulate matter emission modelling based on soot and SOF from direct injection diesel engines," *Energy Conversion and Management*, vol. 48, no. 2, pp. 510-518, Feb. 2007.

[9] B. H., "Physical characterization of particulate emissions from diesel engines: a review," *Journal of Aerosol Science*, vol. 36, no. 7, pp. 896-932, Jul. 2005.

[10] N. Bukowiecki et al., "Iron, manganese and copper emitted by cargo and passenger trains in Zürich (Switzerland): Size-segregated mass concentrations in ambient air," *Atmospheric Environment*, vol. 41, no. 4, pp. 878-889, Feb. 2007.

[11] M. Burkhardt, L. Rossi, M. Boller, "Diffuse release of environmental hazards by railways," *Desalination*, vol. 226, no. 1-3, pp. 106-113, Jun. 2008.

[12] G. D. Pfeifer, R. M. Harrison, and D. R. Lynam, "Personal exposures to airborne metals in London taxi drivers and office workers in 1995 and 1996," *Science of The Total Environment*, vol. 235, no. 1-3, pp. 253-260, Sep. 1999.

[13] A. Seaton, J. Cherrie, M. Dennekamp, K. Donaldson, J. F. Hurley, and C. L. Tran, "The London Underground: dust and hazards to health," *Occupational and Environmental Medicine*, vol. 62, no. 6, pp. 355 -362, Jun. 2005.

[14] P. J. Bolton , P. Clayton, "Rolling—sliding wear damage in rail and tyre steels," *Wear*, vol. 93, no. 2, pp. 145-165, Jan. 1984.

[15] J. F. Archard, "Contact and Rubbing of Flat Surfaces," *Journal of Applied Physics*, vol. 24, p. 981, 1953.

[16] J. C. O. Nielsen, R. Lund□n, A. Johansson, T. Vernersson, "Train-Track Interaction and Mechanisms of Irregular Wear on Wheel and Rail Surfaces," *Vehicle System Dynamics*, vol. 40, pp. 3-54, Jan. 2003.

[17] A. Ward, R. Lewis, R. S. Dwyer-Joyce, "Incorporating a railway wheel wear model into multi-body simulations of wheelset dynamics," in *Tribological Research and Design for Engineering Systems Proceedings of the 29th Leeds-Lyon Symposium on Tribology*, vol. 41, Elsevier, 2003, pp. 367-376.

[18] M. Malvezzi, E. Meli, S. Falomi, A. Rindi, "Determination of wheel–rail contact points with semianalytic methods," *Multibody System Dynamics*, vol. 20, pp. 327-358, Sep. 2008.

[19] J. Tomas, "Prediction of wheel profile wear—comparisons with field measurements," *Wear*, vol. 253, no. 1-2, pp. 89-99, Jul. 2002.